A new lactoferrin- and iron-dependent lysosomal death pathway is induced by benzo[a]pyrene in hepatic epithelial cells.

Morgane Gorria, Xavier Tekpli, Mary Rissel, Odile Sergent, Laurence Huc, Nina Landvik, Olivier Fardel, Marie-Thérèse Dimanche-Boitrel, Jørn A. Holme, Dominique Lagadic-Gossmann

Available online at www.sciencedirect.com
ScienceDirect
Toxicology and Applied Pharmacology 228 (2008) 212–224
Toxicology and Applied Pharmacology
www.elsevier.com/locate/ytaap

A new lactoferrin- and iron-dependent lysosomal death pathway is induced by benzo[*a*]pyrene in hepatic epithelial cells

Morgane Gorria [a,b], Xavier Tekpli [a,b], Mary Rissel [a,b], Odile Sergent [c], Laurence Huc [a,b], Nina Landvik [d], Olivier Fardel [a,b], Marie-Thérèse Dimanche-Boitrel [a,b], Jørn A. Holme [d], Dominique Lagadic-Gossmann [a,b,*]

[a] *Inserm U620; Group « Toxicity of polycyclic aromatic hydrocarbons » (Equipe Labellisée Ligue contre le Cancer); 2 av Pr. Léon Bernard, 35043 Rennes cedex, France*
[b] *Université Rennes 1; IFR140 ; 2 av Pr. Léon Bernard, 35043 Rennes cedex, France*
[c] *UPRES EA 3891, UFR des Sciences Pharmaceutiques et Biologiques, Université de Rennes 1, 2, av. Pr. Léon Bernard, 34043 Rennes cedex, France*
[d] *Division of Environmental Medicine, Norwegian Institute of Public Health, P.O. Box 4404 Nydalen, N-0403 Oslo, Norway*

Received 10 October 2007; revised 3 December 2007; accepted 14 December 2007
Available online 3 January 2008

Abstract

While lysosomal disruption seems to be a late step of necrosis, a moderate lysosomal destabilization has been suggested to participate early in the apoptotic cascade. The origin of lysosomal dysfunction and its precise role in apoptosis or apoptosis-like process still needs to be clarified, especially upon carcinogen exposure. In this study, we focused on the implication of lysosomes in cell death induced by the prototype carcinogen benzo[*a*]pyrene (B[*a*]P; 50 nM) in rat hepatic epithelial F258 cells. We first demonstrated that B[*a*]P affected lysosomal morphology (increase in size) and pH (alkalinization), and that these changes were involved in caspase-3 activation and cell death. Subsequently, we showed that lysosomal modifications were partly dependent on mitochondrial dysfunction, and that lysosomes together with mitochondria participate in B[*a*]P-induced oxidative stress. Using two iron chelators (desferrioxamine and deferiprone) and siRNA targeting the lysosomal iron-binding protease lactoferrin, we further demonstrated that both lysosomal iron content and lactoferrin were required for caspase-3 activation and apoptosis-like cell death.

Keywords: Lysosomes; Apoptosis; Lactoferrin; Iron; Oxidative stress; Carcinogens

Introduction

Lysosomes are intracellular organelles essential for the occurrence of cell death processes triggered by various cellular insults. The lysosomal rupture in necrotic cells is considered to be followed by a massive leakage of proteases into the cytoplasm. Their role during apoptosis appears to rely upon a more gentle membrane destabilization, which leads to a limited release of lysosomal content possibly initiating the apoptotic cascade (for reviews, see Brunk et al. (2001); Ferri and Kroemer (2001)). Lysosomal leakage has been implicated in apoptosis induced by diverse stimuli which includes, drugs (Paquet et al., 2005), TNF-α (Taha et al., 2005), Fas ligation (Brunk and Svensson, 1999), as well as growth factor starvation, possibly mediated through oxidative stress (Brunk and Svensson, 1999) and/or p53 activation (Yuan et al., 2002). Lysosomal disruption can then trigger apoptosis through the translocation of lysosomal proteases into the cytosol, leading to the cleavage of Bid (Cirman et al., 2004), cytochrome *c* release (Zhao et al., 2003; Kessel et al., 2000) and formation of reactive oxygen species (ROS). Regarding this latter aspect, lysosomal destabilization has been recognized as a

Abbreviations: α-NF, α-naphthoflavone; 3-MA, 3-methyladenine; AhR, aryl hydrocabon receptor; AO, acridine orange; B[*a*]P, benzo[*a*]pyrene; BFM, bafilomycin A1; CYP1, cytochrome P450 1; DFO, desferrioxamine; DHE, dihydroethidium; DPO, deferiprone; LFR, lactoferrin; LLoMe, Leucine-Leucyl-*O*-Methyl HBr; NHE1, Na^+/H^+ exchanger 1; PAHs, polycyclic aromatic hydrocarbons; PFT-α, cyclic pifithrin-alpha; pH_i, intracellular pH; ROS, reactive oxygen species; TMA-DPH, trimethylamino-diphenylhexatriene.

* Corresponding author. Inserm U620, Université Rennes 1, Faculté de Pharmacie, 2 av Pr. Léon Bernard, 35043 Rennes cedex, France. Fax: +33 223234794.
E-mail address: dominique.lagadic@rennes.inserm.fr (D. Lagadic-Gossmann).

0041-008X/$ - see front matter © 2008 Elsevier Inc. All rights reserved.
doi:10.1016/j.taap.2007.12.021

common feature of oxidative stress-induced cell damage (Persson et al., 2003; Zdolsek and Svensson, 1993). Thus, lysosomal dysfunction is no longer considered as only a late event of destruction, but also as an initiator step in the apoptotic cascade. The specific leakage of lysosomal proteases may either directly activate caspases (Vancompernolle et al., 1998; Ishisaka et al., 1999), or indirectly after the subsequent release of cytochrome *c* from mitochondria (Vancompernolle et al., 1998; Zang et al., 2000). Furthermore, some lysosomal proteases, including cathepsins, can substitute for caspases in a number of apoptotic models, thereby eliciting caspase-independent apoptotic processes (reviewed in Turk et al. (2002); Broker et al. (2005)). Another cell death process which appears to require lysosomal proteases is autophagy (Kroemer and Jaattela, 2005), although the relative impact of autophagy in cell death as such is still a matter of debate (Baehrecke, 2005; Hait et al., 2006).

Whereas the involvement of lysosomes in cell death is now commonly accepted, the origin of their dysfunction and their role during cell death processes needs to be further characterized. ROS have been shown to induce lysosomal leakage (Brunk et al., 1997; Roberg et al., 1999), possibly as a consequence of intralysosomal iron-catalyzed oxidative processes, more specifically lipid peroxidation (Persson et al., 2003; Dare et al., 2001). It has been shown that an increase in lysosomal membrane fluidity may elicit both an increase in osmotic sensitivity (Yang et al., 2000), an increase in proton permeability (Wan et al., 2002), and a decrease in potassium permeability (Wang and Zhang, 2005). Thus, various stimuli can induce changes in lysosomal membrane fluidity (Mozhenok et al., 1998; Myers et al., 1991); regarding that point, it is worth noting that some apoptotic insults can trigger changes in composition and fluidity of both plasma membrane and intracellular organelle membranes (Singh et al., 1996).

Polycyclic aromatic hydrocarbons (PAHs) are important environmental pollutants, to which humans are largely exposed. In addition to their well-known carcinogenic effects, PAHs may also induce apoptosis in various cell types, which includes some hepatic cell lines (Solhaug et al., 2004; Huc et al., 2004). Recently we showed that a low concentration of the prototype PAH, benzo[*a*]pyrene (B[*a*]P; 50 nM), induced an apoptosis-like cell death in the rat hepatic epithelial F258 cell line, through multiple pathways. In addition to the activation of the p53 apoptotic pathway, we evidenced that H_20_2 produced during B[*a*]P metabolism was responsible for an early NHE1 activation which resulted in intracellular alkalinization. We further showed that both p53 and NHE1 pathways induced mitochondrial dysfunction, responsible for a late phase of ROS production and secondary intracellular acidification (Huc et al., 2004, 2006, 2007). Interestingly, we also evidenced an acidification- and cathepsin B-dependent activation of the endonuclease LEI/L-DNase II (Huc et al., 2006). Furthermore, we found that membrane fluidization and iron uptake constituted two important events in this cell death process (Gorria et al., 2006a,b). Moreover, B[*a*]P *per se* has been described to directly interact with membranes (Jimenez et al., 2002), and the aryl hydrocarbon receptor (AhR), a key component of PAH-induced responses (Billiard et al., 2006), may be a putative modifier of lysosomal permeability (Caruso et al., 2004, 2006). We then decided to look for possible lysosomal changes upon B[*a*]P exposure in F258 cells, and to test their involvement in the related apoptosis-like cell death process. In the present study, our data clearly showed that B[*a*]P (50 nM) induced modifications of lysosomes and that these were involved in the cell death process, notably by regulating the activation of caspase-3 through an iron- and lactoferrin-dependent step.

Materials and methods

Chemicals. B[*a*]P, α-naphthoflavone (α-NF), 3-methyladenine (3-MA), bafilomycin A1 (BFM), oligomycin, and desferrioxamine (DFO) were all purchased from Sigma-Aldrich (Saint Quentin Fallavier, France). Deferiprone (DPO; 1,2-dimethyl-3-hydroxy-4-pyridone) was obtained from Acros (Acros Organics, Noisy Le Grand, France). Z-FA-FMK and Z-FY-CHO were purchased from Santa Cruz (Santa Cruz Biotechnology, Tebu-bio SA, Le Perray en Yvelynes, France). Leucine-Leucyl-*O*-Methyl HBr (LLoMe) was purchased from Bachem (St. Helens, UK). Cyclic pifithrin-alpha (PTF-α) was purchased from Calbiochem (France Biochem, Meudon, France).

Cell culture and treatment. As previously described (Huc et al., 2004), F258 cells were grown in Williams' E Medium (Gibco Invitrogen Corporation, Paisley, Scotland, UK) supplemented with 10% fetal calf serum (FCS), 5 units/mL of penicillin, 0.5 mg/mL streptomycin and 2 mM L-Glutamine in a humidified atmosphere, in 5% CO_2 at 37 °C. F258 cells, growing in exponential phase, were treated 24 h following seeding (at 2.5×10^3 cells/cm^2) with 50 nM or 5 μM B[*a*]P and/or the different inhibitors tested (applied to cells 2 h prior to B[*a*]P exposure) for various treatment times.

Cell ultrastructure. Cells were fixed by dropwise addition of glutaraldehyde and analysed according to standard conditions. After fixation, the specimens were rinsed several times with PBS followed by postfixation with 1% osmium tetroxide in phosphate buffer for 1 h. After a further rinsing with PBS for 15 min, the tissue specimens were dehydrated through a series of graded ethyl alcohols from 70 to 100%. Cells were then embedded in DMP30 Eponate for 24 h at 60 °C. Thin sections (70 nM) were collected onto cooper grids and counterstained with lead citrate before examination with a Philips transmission electron microscope.

Visualization of lysosomal morphology. After treatment, cells seeded on glass coverslips were labeled using the fluoroprobe LysoTracker (1 μM; Molecular Probes, St Louis), incubated in the culture medium, at 37 °C for 1 h. As positive control, cells were exposed to 1 μM LLoMe (a disrupting lysosome agent) 1 h prior to LysoTracker labelling. After labelling, the coverslips were observed using a fluorescence microscope (Olympus BX60), to detect the emission of red fluorescence (x40). Photographs are representative of three independent experiments.

Acridine orange (AO) lysosomal labelling. Lysosomal integrity was analysed using the lysosomotropic weak base acridine orange (AO, 5 μM; Molecular Probes), a metachromatic fluorophore that accumulates in normal lysosomes, turning red under blue excitation light. When AO-loaded lysosomes are damaged, AO is then released to the cytosol, turning green under blue excitation light. The amount of red (FL-3) fluorescence in AO-labeled cells reflects the amount (number and size) of intact lysosomes, while increased green (FL-1) cytosolic fluorescence reflects lysosomal damage (Uchimoto et al., 1999).

After 48 or 72 h of treatment, cells, both adherent and floating, were collected and loaded with AO (5 μM) for 20 min at 37 °C. Positive control cells were treated with LLoMe (1 μM) for 1 h prior to AO labelling. After washing with ice-cold PBS, cells were finally analysed using a FACSCalibur flow cytometer (Becton-Dickinson, Franklin Lakes, NJ). The illustrated histograms are representative of at least three independent experiments.

Estimation of bulk and vesicular membrane fluidity. Bulk and vesicular membrane fluidity was analysed by a fluorescence polarization technique adapted from Illinger and Kuhry (1994), which uses the TMA-DPH (trimethylamino-diphenylhexatriene; Molecular probes) fluoroprobe.

After 72 h of treatment, cells were collected and labeled with TMA-DPH (1 μM) for 30 min at 37 °C. Labeled cells were then separated in two eppendorf tubes, centrifuged, harvested and the pellet was conserved on cold ice until polarization measurement. Just before measurement with a Perkin Elmer LS 50B spectrofluorimeter equipped for polarization, cells were resuspended either in ice-cold PBS to wash the probe present in plasma membrane (*eppendorf 1*: only intracellular vesicles [endosomes and lysosomes] were labeled), or ice-cold TMA-DPH 1 μM (*eppendorf 2*: both membrane and vesicles were labeled). The measurements were performed at 4 °C, using the following setups, λ_{exc}=360 nM; $slit_{exc}$=5 nM; λ_{em}=430 nM; $slit_{em}$=10 nM; polarization ratio $r=(I_{VV}-G*I_{VH})/(I_{VV}+G*I_{VH})$ with $G=I_{HV}/I_{HH}$. Histograms show an experiment representative of three.

Measurement of lysosomal pH. Changes in lysosomal pH were analysed using the fluorescent probe LysoSensor Yellow/Blue DND-160 (Molecular Probes), which localizes exclusively within the lysosomes and shows a dual emission when excited under UV light (360 nM), sensitive to pH (Lin et al., 2005). After a 72 h-treatment, cells grown on coverslips were loaded with 1 μM LysoSensor for 5 min at room temperature, washed with PBS and observed under a fluorescence microscope. Under our experimental conditions, a shift of fluorescence to the yellow color corresponds to a change of pH towards more alkaline values, as confirmed upon an acute treatment with bafilomycin A1, a known inhibitor of lysosomal H^+-ATPase (Tapper and Sundler, 1995). Photographs are representative of three independent experiments.

Visualization of chromatin fragmentation. After treatment, both adherent and floating F258 cells were collected, centrifuged and incubated with the nuclear dye Hoechst 33342 (0.5 μg/mL; Molecular Probes, Leiden, Holland) in PBS, at room temperature for 15 min. The percentage of apoptotic cells was determined by UV fluorescence microscopy (Olympus BX60), counting nuclei with condensed or fragmented chromatin (*i.e.* morphology corresponding to late apoptotic cells) beyond a total of a minimum of 200 nuclei counted (normal and apoptotic). At least three independent experiments were performed per condition tested.

Measurement of effector caspase-3 activity. Caspase activity assay has been previously described (Gilot et al., 2002). Briefly, both adherent and floating F258 cells were lysed in the caspase activity buffer. 40 μg of crude cell lysate was incubated with 80 μM DEVD-AMC for 2 h at 37 °C. Caspase-mediated cleavage of DEVD-AMC was measured by spectrofluorimetry (Spectramax Gemini, Molecular Devices, Sunnyvale, CA, USA) at the excitation/emission wavelength pair of 380/440 mm. Three independent experiments, performed in triplicate, were carried out for each experimental condition.

Covalent-binding of B[a]P. The amount of B[*a*]P covalently bound to macromolecules was determined as previously described (Solhaug et al., 2005). In short, F258 cells were incubated with 50 nM ^{3}H-B[*a*]P (76 Ci/mmol, 5 mCi/mL, Isobio, Fleurus, Belgium) for 7 h in the absence or presence of either PFT-α (30 μM) or BFM (5 nM or 10 nM). The reactions were stopped by placing the dishes on ice. The cells were then scraped off and protein precipitated with trichloroacetic acid. The precipitates were washed sequentially with trichloroacetic acid, methanol and ethanol:ether (1:1). The amount of radioactivity covalently bound to macromolecules was determined by scintillation counting. Protein concentration was measured using a BioRad DC protein assay kit. Results, expressed as percent of vehicle control, are given as means of three independent experiments.

Reactive oxygen species (ROS) production. ROS production was detected using the oxidation-sensitive fluorescent probe dihydroethidium (DHE, Molecular Probes). After 48 or 72 h of treatment, cells, both adherent and floating, were collected and loaded with DHE (5 μM) for 20 min at 37 °C. Positive control cells were treated with menadione during the 20 min-incubation time with DHE. Cells were then washed with ice-cold PBS and analysed using a FACSCalibur flow cytometer. The illustrated histograms are representative of three independent experiments. Results are also given as a bar graph of the mean±standard error of differences in fluorescence intensity between control and B[*a*]P-treated cells.

Analysis of lipid peroxidation. Lipid peroxidation was measured using the fluoroprobe C_{11}-BODIPY$^{581/591}$ (4,4-difluoro-5- [4-phenyl-1,3-butadienyl] -4-bora-3a,4a-diaza-*s*-indacine-3-undecanoic acid; Molecular Probes), as previously described (Gorria et al., 2006a). At least three independent experiments were performed per condition tested.

Measurement of pH_i. The pH_i of F258 cells cultured on glass coverslips was monitored using the pH-sensitive fluoroprobe, carboxy-SNARF-1 (carboxy-seminaphtorhodafluor; Molecular Probes), as previously described (Huc et al., 2004). At least three independent experiments were performed per condition tested.

Transfection and small interfering RNAs (siRNA). siRNA oligonucleotides directed against Lactoferrin (SMART pool of 4 siRNA; M-081373-00) and Non Targeting siRNA (si control; D-001210-01) were purchased from Dharmacon (Perbio Science France, Brebieres, France). Transfections of siRNA were performed in 60 mm dishes on 90% confluent F258 cells, using TransFectin lipid reagent (BioRad, France). Per dish, 250 pmol siRNA and 12.5 μL TransFectin lipid reagent were applied in a final volume of 2 mL Opti-MEM for 4 h. Cells were then passaged in low-serum containing medium (*i.e.* Williams' medium complemented with glutamine, penicillin/streptomycin and 2% decomplemented FCS) in order to avoid lactoferrin supplementation by serum. Cells were treated with 5 μM B[*a*]P during exponential phase for 48 h, corresponding to the apoptotic steps observed at 72 h when treated with 50 nM B[*a*]P.

Reverse transcription-PCR. Total RNA was purified in Trizol™ (Invitrogen). The complementary DNA was synthesized from 5 μg total RNA using the designed oligo dT15V(GAC) (100 pmol/μL) and Superscript™ RNase H-Reverse Transcriptase kit (GIBCO-BRL, Paisley, UK). cDNA aliquots were amplified using the Master Mix (Promega, Madison, WI) and 0.1 mM of forward and backward gene primers. PCR was carried out with an automated heat block thermal cycler (GeneAmp PCR System 9700, Applied BioSystems, USA). After an initial denaturation at 95 °C, the following PCR profile was used: 30 s at 94 °C, 30 s at 56 °C, 1 min at 72 °C for 30 cycles followed by an elongation step for 7 min at 72 °C. The following primers were used for PCR: 18S sens GG-AAA-GCA-TTT-GCC-AAG-AAT and antisens AG-TCG-GCA-TCG-TTT-ATG-GTC; Lactotransferrin Quantitect® Primers (QUIAGEN Cat No: TC118685). The specificity of PCR products was analysed by electrophoresis on 2% agarose gels and visualized by ethidium bromide. Illustrated gels are representative of three independent experiments.

Statistical analysis. All data are quoted as mean±standard error of *n* independent experiments. Analysis of variance followed by Newman–Keuls test was used to analyse the statistical significance of differences between treatments. Differences were considered significant at the level of $p<0.05$.

Results

Changes in cell ultrastructure and lysosomal morphology upon B[a]P exposure

The purpose of our initial experiments was to observe the appearance of degradation vesicles, such as autophagosomes, in F258 cells treated with B[*a*]P using electron microscopy. As shown in Fig. 1A, a 72 h-treatment with 50 nM of B[*a*]P induced the appearance of vesicles with a dense content possibly containing degraded cellular material. The observation that a double membrane was present in some of these vesicles was suggestive of autophagosomes (Eskelinen, 2005). This led us to hypothesize that lysosomes might be involved in the deleterious B[*a*]P effects. To further test the possibility that lysosome size and/or integrity were affected in F258 cells treated with 50 nM of B[*a*]P for 24, 48 and 72 h, we first used the fluoroprobe LysoTracker. As illustrated in Fig. 1B, B[*a*]P induced an increase

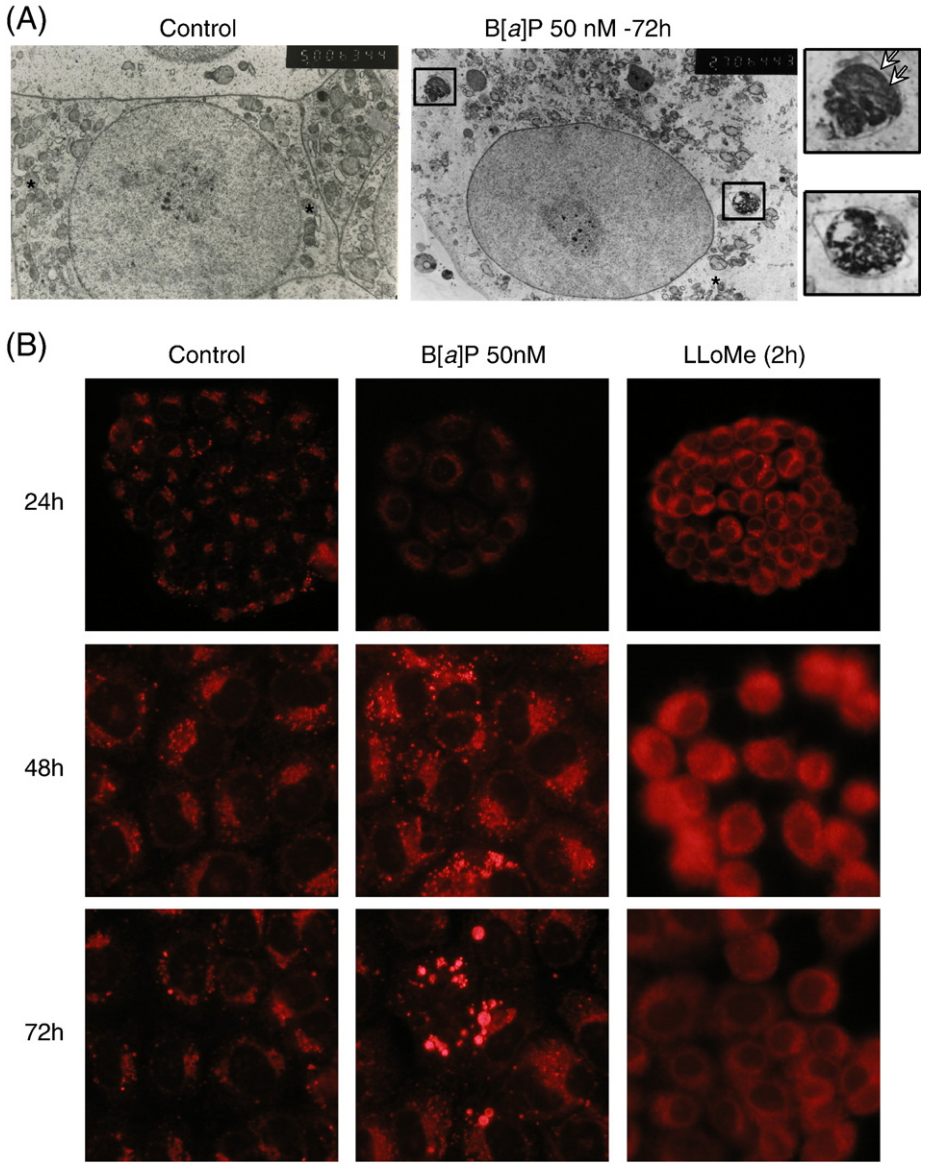

Fig. 1. Effects of B[*a*]P on cell (A) and lysosomal (B) morphology in F258 cells. Cells were treated or not (control) with B[*a*]P (50 nM) for either 72 h (A) or for 24, 48 or 72 h (B). (A) After fixation, cells were analysed by electron microscopy. The right hand side images correspond to a higher magnification of the intracellular vesicles observed upon B[*a*]P treatment. White arrows: double membrane in vesicles; black asterisk: mitochondria. (B) After collection, cells were stained with the fluoroprobe LysoTracker and analysed by fluorescence microscopy. Punctuate red spots correspond to lysosomes with intact integrity. The red diffuse staining observed upon the positive control LLoMe (1 mM; 1 h) exposure, reflects total rupture of lysosomes.

in lysosome size starting at 48 h, with marked effects at 72 h. The lysosomotropic agent LLoMe which induces a rupture of lysosomal membranes, is used as a positive control of loss of membrane integrity. A diffuse cell staining is visualized after acute treatment by LLoMe; whereas B[*a*]P-treated cells did not show this pattern, suggesting that B[*a*]P does not induce any loss of lysosomal membrane integrity.

Lysosomes were then analysed by flow cytometry after labelling with the lysosomotropic base acridine orange (AO), as described in Materials and methods. We observed that B[*a*]P (50 nM) induced an increase in FL-3 fluorescence following 48 and 72 h of treatment (rightward shift of fluorescent peak; Figs. 2A and B); this thus confirmed the increase in the size of lysosomal compartment upon B[*a*]P exposure. When looking at the FL-1 peaks, it was clear that B[*a*]P elicited only late effects *i.e.* after 72 h of treatment (Figs. 2A and B), also suggesting a near absent, early loss of lysosomal integrity. As shown by the dotted peak in Figs. 2A and B, the positive control LLoMe induced a leftward shift of FL-3 peak compared to control (*i.e.* a decrease in the amount of intact lysosomes), and a rightward shift in FL-1 (*i.e.* an increase in leakage of AO into the cytoplasm), as expected. Furthermore, using α-naphthoflavone (α-NF; 10 μM) to inhibit B[*a*]P metabolism *via* CYP1, we found that the effects of B[*a*]P on AO fluorescence were fully inhibited, thus indicating that B[*a*]P metabolism was involved in these effects.

We have previously shown that B[*a*]P (50 nM) increased bulk membrane fluidity (at the inner layer) from 48 h of treatment

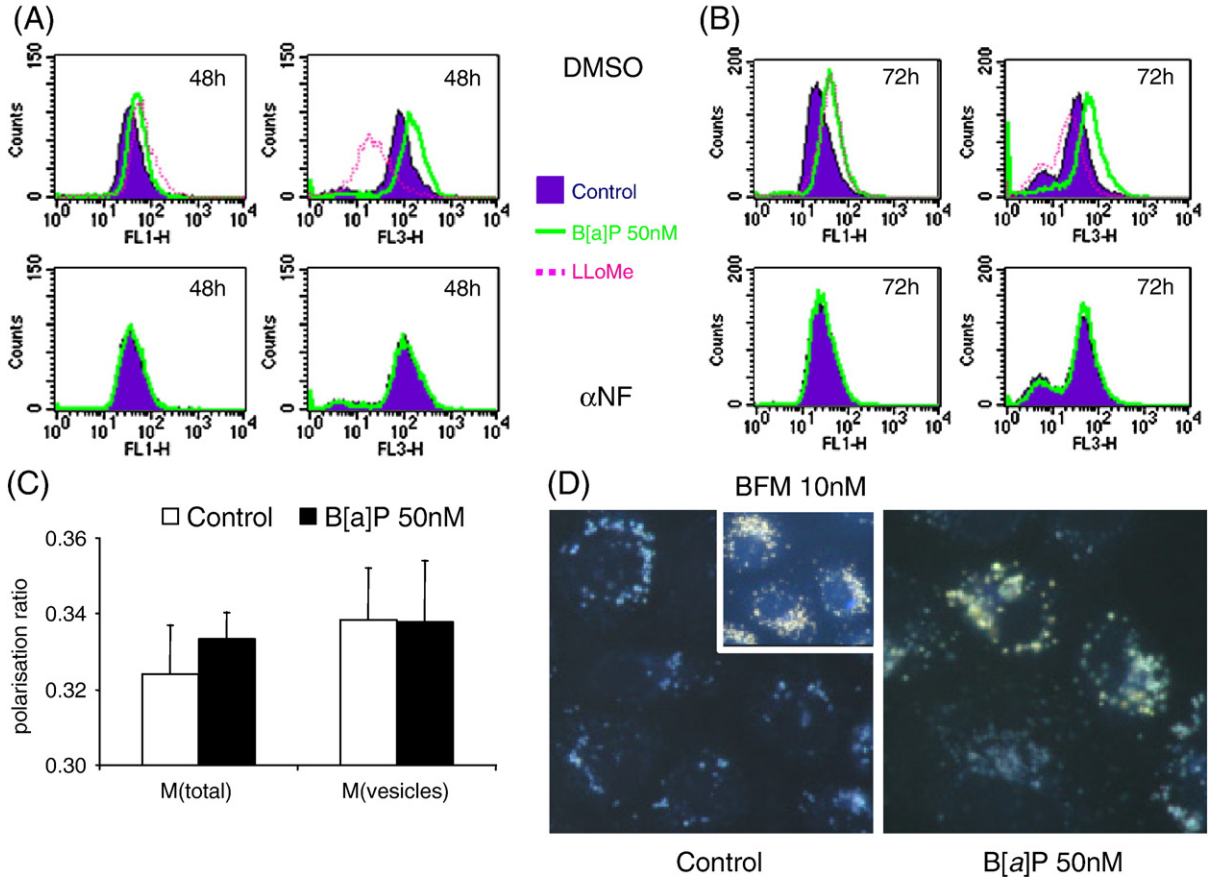

Fig. 2. Characterization of lysosomal alterations in B[*a*]P-treated cells. (A, B) F258 cells were treated or not (control) with B[*a*]P (50 nM) in the presence (lower histograms) or not (upper histograms) of α-naphthoflavone (α-NF; 10 μM; to inhibit metabolism of B[*a*]P) for 48 (A) or 72 h (B). Cells were then stained with the fluoroprobe acridine orange (AO) and analysed by flow cytometry. LLoMe (1 mM, 1 h) was used as positive control. Histograms are representative of 3 independent experiments. (C) Fluidity of either bulk membranes [M(total)] or intracellular vesicles [M(ensosomes)] was determined from cells treated or not with B[*a*]P for 72 h using TMA-DPH and a polarization fluorescence technique. Data are given as mean±S.E.M. of 3 independent experiments. (D) Lysosomal pH was analysed by fluorescence microscopy in cells stained with LysoSensor Yellow/Blue DND-160 following or not treatment with B[*a*]P (72 h).The inset correspond to cells treated with bafilomycin A1 (BFM; 10 nM, 30 min), a known inhibitor of vacuolar H^+-ATPase. Photographs are representative of 3 independent experiments.

(Gorria et al., 2006b). In order to examine if fluidity of lysosome membrane was sensitive to B[*a*]P exposure, a protocol based on the use of TMA-DPH and polarization fluorescence measurement was applied to cells. This protocol allowed the determination of the outer layer fluidity of membranes from the whole cells on one hand and from only intracellular vesicles (endosomes and lysosomes) on the other hand. As shown in Fig. 2C, B[*a*]P did not induce any significant change in surface membrane fluidity, whatever the compartment tested; indeed the polarization ratio remained unchanged between control and B[*a*]P-treated cells in both cases.

Since no significant changes in physical properties (rupture or outer fluidization) of lysosomal membranes were observed following B[*a*]P treatment, we then wondered whether the lysosomal pH was affected. Using the LysoSensor Yellow/Blue DND-160 probe, we found that B[*a*]P (50 nM; 72 h) induced a dramatic shift in the color of emitted fluorescence between lysosomes in B[*a*]P-treated cells *vs* control (Fig. 2D); this change was already observed at 48 h, but not at 24 h (not shown). Interestingly, lysosomal pH in B[*a*]P-treated cells was very close to that detected in cells acutely treated with bafilomycin A1 (BFM; 10 nM), an inhibitor of the vacuolar H^+-ATPase previously shown to alkalinize lysosomes (Heming et al., 1995).

Altogether, the present data clearly indicated that B[*a*]P treatment induced alterations of lysosomes in F258 cells, with an increase in the size of lysosomal compartment associated with an alkaline shift of its pH.

Lysosomes are involved in B[a]P-induced cell death

Since B[*a*]P induced lysosome alterations in F258 cells, we then looked for any possible role for these changes in the related cell death by using BFM, an inhibitor of the lysosomal pathway (Bidere et al., 2003; Boya et al., 2003). We found that co-treatment with BFM (5 and 10 nM) and B[*a*]P (50 nM) significantly inhibited both the amount of cells exhibiting nuclear fragmentation (as detected by Hoechst staining; Fig. 3A) and caspase-3 activity (Fig. 3B), these effects being more pronounced at 10 nM BFM. As can be seen from the data presented in Fig. 3B, BFM used at 10 nM was capable of fully inhibiting B[*a*]P-induced caspase-3 activity. This suggested either a strong involvement of lysosomes in the activation of this protease, or a

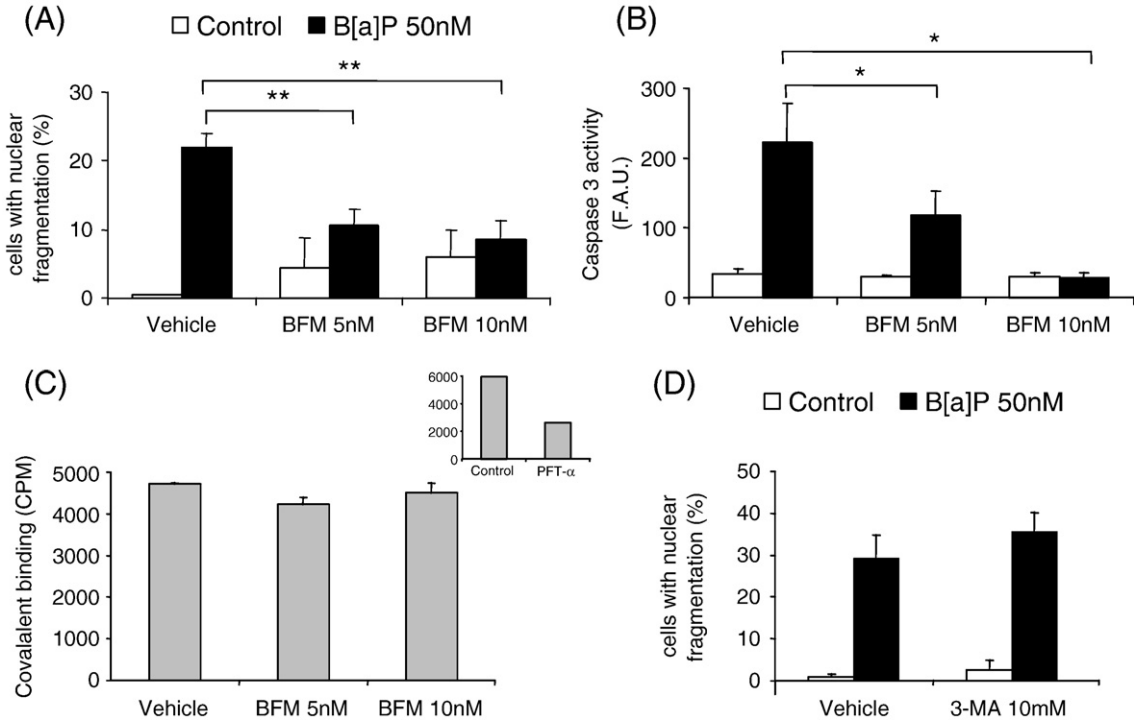

Fig. 3. Involvement of lysosomal alterations in B[*a*]P-induced cell death in F258 cells. (A, B) F258 cells were treated or not (control) with B[*a*]P (50 nM) in the presence (BFM) or not (vehicle: DMSO) of bafilomycin A1 (5 or 10 nM) for 72 h. (A) The percentage of cells with apoptosis-like features was analysed after Hoechst 33342 staining. $^{**}p<0.01$. (B) Caspase activity was measured by spectrofluorimetry following a 72 h-treatment. $^{*}p<0.05$. F.A.U.: Fluorescence Arbitrary Units. (C) The effects of BFM (5 and 10 nM) were tested on B[*a*]P metabolism through determination of the amount of ^{3}H-B[*a*]P covalently bound to macromolecules. As positive control, pifithrin-α (PFT, 30 μM), a known inhibitor of B[*a*]P metabolism was tested (inset). (D) Cells were treated or not (control) with B[*a*]P (50 nM) in the presence (3-MA) or not (vehicle: DMSO) of 3-methyladenine (10 mM; a known inhibitor of autophagy) for 72 h. The percentage of cells with apoptosis-like features was analysed using Hoechst 33342 staining. $N=3$–4 independent experiments for all the protocols.

non specific effect of BFM (*i.e.* an inhibition of B[*a*]P metabolism, as already observed with other so-called specific inhibitors (Solhaug et al., 2005)). However, analysis of radioactive B[*a*]P enabled us to conclude that the activation of B[*a*]P into reactive metabolites (covalently bound to macromolecules) was not inhibited by BFM, as no significant change was observed between B[*a*]P-treated and B[*a*]P+BFM-treated cells (Fig. 3C). In cells co-treated with PFT-α, an inhibitor of p53 previously shown to also inhibit the metabolic activation of B[*a*]P (Solhaug et al., 2005; Sparfel et al., 2006), a clear inhibition of covalent binding was observed (about 50%; inset).

As BFM has previously been reported to prevent autophagy (Kanzawa et al., 2004) and since autophagosome-like vesicles were detected upon B[*a*]P in our model (Fig. 1A), we decided next to further examine any possible role of autophagy. To this aim, we used 3-methyladenine, a known inhibitor of this process (Jia et al., 1997). As illustrated in Fig. 3D, no decrease of the percentage of cells with nuclear fragmentation was detected.

Taken together, these results therefore point to the involvement of lysosomes in the cell death cascade induced by B[*a*]P, but apparently independent of an autophagic process.

Crosstalks between lysosomal compartment and mitochondrion during B[a]P-induced cell death cascade

It has been suggested that lysosomal alterations may occur upstream mitochondrial dysfunction (Roberg et al., 1999; Yin et al., 2005). In order to test this putative link in our model, we analysed the effect of BFM on two B[*a*]P-induced, mitochondria-dependent events, namely ROS production and intracellular acidification (Huc et al., 2004). As shown in Fig. 4A, mitochondrial ROS production induced by B[*a*]P (50 nM) was not inhibited by BFM (10 nM); indeed, co-treatment with BFM did not prevent the B[*a*]P-induced rightward shift of FL-2 DHE fluorescence, regardless of treatment time. Regarding mitochondria-related acidification detected following 72 h of treatment (Fig. 4B), BFM (10 nM)+B[*a*]P-treated cells still exhibited a significantly lower pH than BFM-treated cells, suggesting that BFM was not effective to inhibit acidification in B[*a*]P-treated cells. We also quantified the B[*a*]P-induced oxidative stress by measuring lipid peroxidation following a 72 h-treatment. As illustrated in Fig. 4C, co-treating cells with both BFM (10 nM) and B[*a*]P markedly inhibited lipid peroxidation, suggesting that lipid peroxidation was partly dependent on lysosomal damages.

To further study the possible crosstalk between mitochondria and lysosomes, we decided to test whether mitochondrial damage might result in lysosomal dysfunction. Oligomycin, an inhibitor of mitochondrial F_0-F_1 H^+-ATPase, has previously been found to block cell death in our model (Huc et al., 2007). As seen in Fig. 4D, the addition of oligomycin prevented lysosomal alterations as evidenced by the inhibition of the B[*a*]P-induced rightward shift in FL-3 AO fluorescence. This suggested that mitochondrial dysfunction induced by B[*a*]P might be responsible for lysosomal alterations.

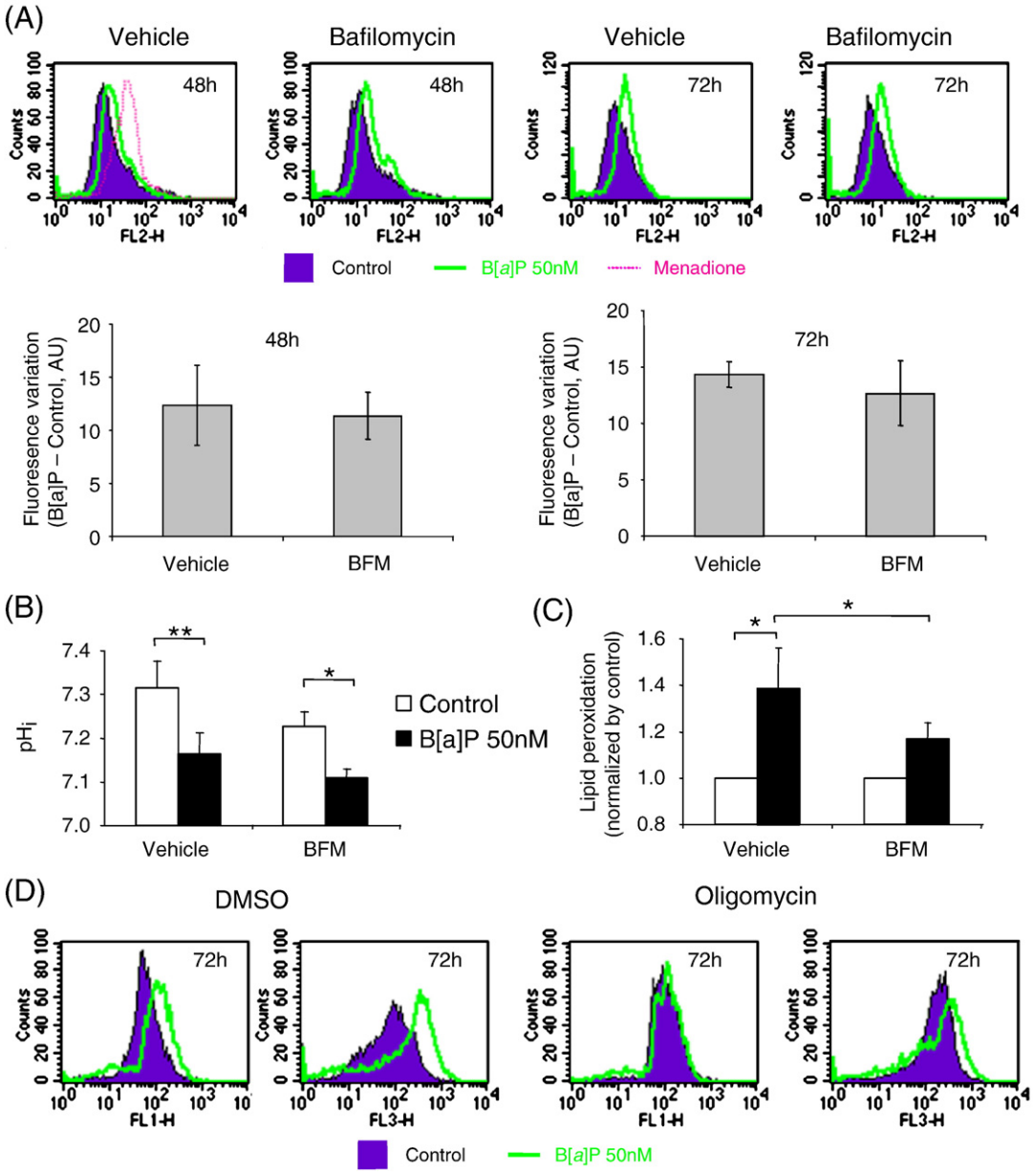

Fig. 4. Lysosomal alterations stem from mitochondrial dysfunction induced by B[*a*]P. (A, B, C) Effects of inhibiting lysosomal alterations by bafilomycin A1 (BFM, 10 nM) on mitochondrial dysfunction induced by B[*a*]P (50 nM). (A) The mitochondria-dependent $O_2^{\cdot-}$ production was recorded from F258 cells treated with B[*a*]P for 48 or 72 h in the presence or not of bafilomycin A1 using DHE and flow cytometry. A 20 min-treatment with menadione was used as positive control. Differences in DHE fluorescence between control and B[*a*]P-treated cells, in the presence (BFM) or not (vehicle) of bafilomycin, were calculated and are given in the bar graph. (B) Effects of BFM on the pH_i decrease induced by B[*a*]P (50 nM) in F258 cells following 72 h of treatment. $*p<0.05$, $**p<0.01$. (C) Effects of BFM on the lipid peroxidation from F258 cells treated with B[*a*]P for 72 h (results are expressed relatively to corresponding control, B[*a*]P-untreated cells for each condition). $*p<0.05$. In panels (B) and (C), vehicle corresponds to DMSO-treated, BFM-untreated cells. (D) Effects of inhibiting mitochondrial dysfunction with oligomycin (8 μM; a known F_0F_1-ATPase) on lysosomal alterations induced by a 72 h-treatment with B[*a*]P (50 nM). Cells were stained with acridine orange (AO) and analysed by flow cytometry. $N=3$ independent experiments for all the protocols tested.

Involvement of iron in caspase activation

Following the demonstration that lysosomes were important for B[*a*]P to induce cell death in F258 cells, we finally sought the mechanisms underlying such an implication. Lysosomes constitute the cellular compartment containing the largest fraction of low molecular weight iron (Petrat et al., 2001). Moreover, due to their acidic pH, these organelles exhibit the perfect environment for Fenton-type reactions leading to oxidative stress and lipid peroxidation (Schafer and Buettner, 2000). Chelating the lysosomal iron content may then be a way to decrease oxidative stress during cell death such as apoptosis (Yu et al., 2003).

In this context, in order to evaluate the importance of the specific lysosomal iron content, two iron chelators with different intracellular localization were used: desferrioxamine (DFO), which is not capable of entering cells by passive diffusion and is hence mostly located within the late endosomes and lysosomes after endocytosis (Glickstein et al., 2005), and deferiprone

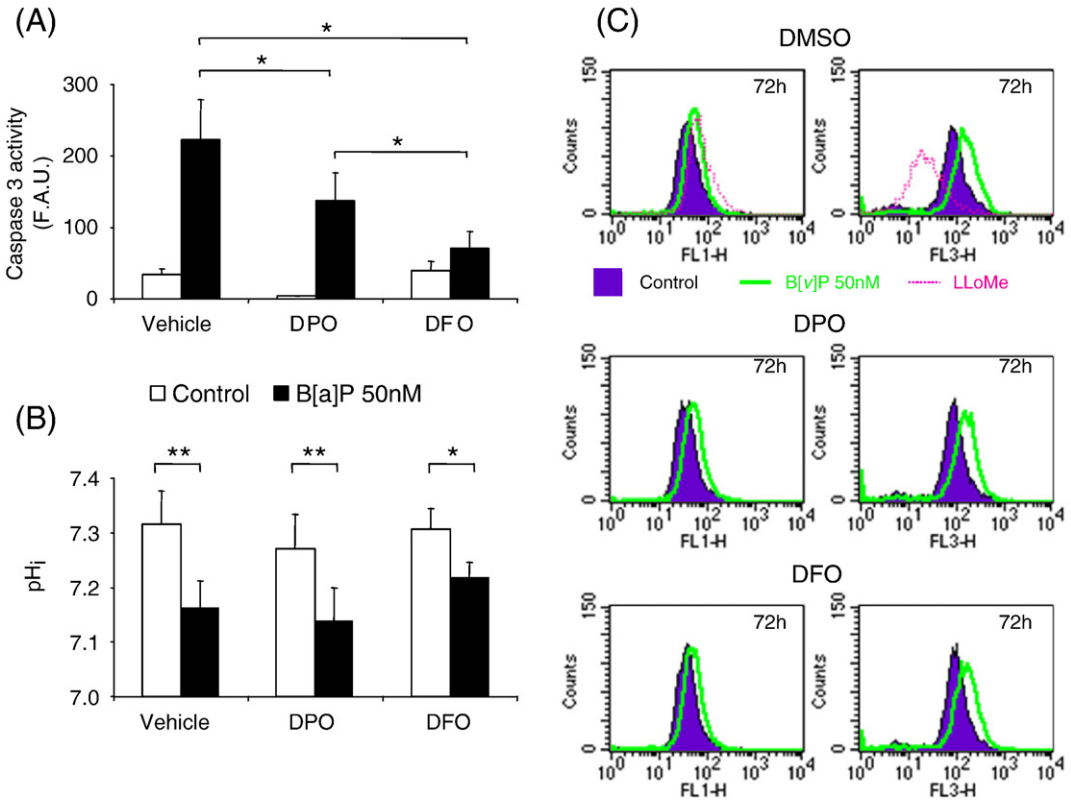

Fig. 5. Effects of iron chelation on different steps of the apoptotic cascade induced by B[*a*]P in F258 cells. (A, B, C) F258 cells were treated or not (control) with B[*a*]P (50 nM) in the presence or not (vehicle: DMSO) of either deferiprone (DPO, 60 μM) or desferrioxamine (DFO, 4 μM) for 72 h. (A) Caspase activity was measured by spectrofluorimetry. $*p<0.05$. F.A.U.: Fluorescence Arbitrary Units. (B) Effects of DFO or DPO on the pH_i decrease induced by B[*a*]P (50 nM) in F258 cells following 72 h of treatment. $*p<0.05$, $**p<0.01$. (C) Effects of DFO or DPO on lysosomal dysfunction as detected by acridine orange staining (AO) following 72 h of treatment. LLoMe (1 mM; 1 h): positive control. $N=3$ independent experiments for all the protocols tested.

(DPO). Our previous work showed that these two chelators significantly reduced the percentage of cells with fragmented nucleus as well as lipid peroxidation elicited by B[*a*]P exposure (Gorria et al., 2006a). After checking that DFO and DPO were ineffective on B[*a*]P metabolism (data not shown), we decided to further focus on the effects of these molecules on cell death, especially by looking at caspase-3 activity, (which was fully inhibited by BFM). As shown in Fig. 5A, both chelators inhibited the B[*a*]P-induced increase in caspase-3 activity. From this figure, it was noteworthy that DFO was more potent than DPO, with a near total inhibition of the increase; this therefore strongly suggested the involvement of the lysosomal iron pool in caspase-3 activation by B[*a*]P.

In order to get further insight into the role of this iron pool, we then tested its possible involvement in both the lysosomal and the mitochondrial dysfunction, as already observed by others (Persson, 2005; Persson et al., 2003). However, using AO staining of lysosomes, we observed that neither DFO nor DPO inhibited the B[*a*]P-induced lysosomal dysfunction (Fig. 5C; no inhibition of the shift at 72 h of B[*a*]P treatment). Similarly, regarding mitochondrial dysfunction, the related acidification was also not prevented by the two chelators (Fig. 5B). These results therefore suggested that lysosomal iron was implicated in the cell death cascade downstream lysosomal alterations and mitochondrial dysfunction.

Involvement of lysosomal proteases in caspase-3 activation

Previous study has shown that B[*a*]P-induced acidification was essential for caspase-3 activation (Huc et al., 2006). Furthermore, based upon our results showing a role for lysosomes in B[*a*]P-induced cell death, and a strong inhibition of caspase-3 activation by both BFM and DFO, we finally hypothesized that a lysosomal protease was involved in caspase-3 activation. We focused first on the possible involvement of cathepsins, especially as our previous study has indicated the involvement of a cathepsin B-dependent activation of LEI/L-DNase II in our model (Huc et al., 2006). Using Z-FA-FMK (cathepsin B inhibitor) and Z-FY-CHO (cathepsin L inhibitor), we demonstrated that inhibiting these cathepsins led to a significant decrease of B[*a*]P (50 nM, 72 h)-induced cell death quantified by Hoechst staining (Fig. 6A), thus confirming the involvement of cathepsins in our model. However, no decrease in caspase-3 activation was detected under these conditions, whatever the inhibitor used (Fig. 6B). Therefore, caspase activation upon B[*a*]P exposure appeared not to depend on cathepsins.

Since iron seemed essential for caspase-3 activation in our model, we next focused on an iron-binding lysosomal protease recently shown to be involved in caspase-3 activation, namely lactoferrin (LFR) (Katunuma et al., 2006, 2004). In order to test the involvement of LFR in the cell death induced by B[*a*]P, a

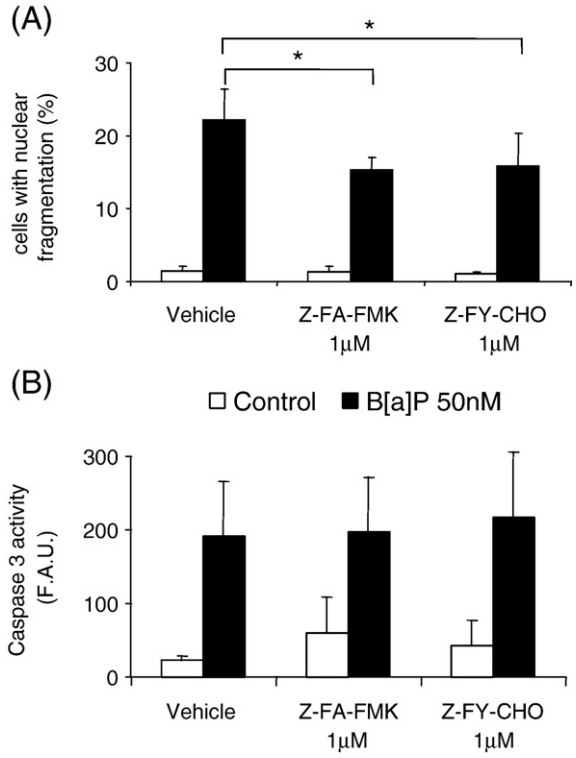

Fig. 6. Cathepsins B and L are involved in B[*a*]P-induced cell death cascade but not in the increase of caspase-3 activity. (A) F258 cells were treated or not (control) with B[*a*]P (50 nM) in the presence or not (vehicle: DMSO) of either Z-FA-FMK (1 μM; to inhibit cathepsin B) or Z-FY-CHO (1 μM; to inhibit cathepsin L) for 72 h. The percentage of apoptotic cells was analysed by Hoechst 33342 staining. *$p<0.05$ (B) Cells were treated or not (control) with B[*a*]P in the presence or not (vehicle) of either Z-FA-FMK or Z-FY-CHO. Caspase activity was measured by spectrofluorimetry following a 72 h-treatment. F.A.U.: Fluorescence Arbitrary Units. $N=3$ independent experiments for all the protocols tested.

transfection protocol with siRNA targeting LFR was applied to cells. As shown in Figs. 7A and B, silencing of LFR expression resulted in a significant decrease of B[*a*]P-induced cell death (by about 40%; Fig. 7A), as well as a near complete inhibition of caspase-3 activation (Fig. 7B). Fig. 7C clearly shows, by using RT-PCR, the efficiency of our protocol to inhibit LFR expression both in control and B[*a*]P-treated cells. Altogether, these results demonstrate the involvement of lactoferrin in caspase-3 activation upon B[*a*]P treatment.

Discussion

Although the involvement of lysosomes in cell death processes has long been ignored, an increased interest has recently appeared, with the demonstration of the role of these organelles in various models of necrosis and apoptosis, induced by stimuli as diverse as oxidative stress (Brunk et al., 1997; Roberg et al., 1999), heavy metal accumulation (Marchi et al., 2004), death receptor ligands (Brunk and Svensson, 1999; Ono et al., 2003) or direct lysosomal disruption (Cirman et al., 2004; Zhao et al., 2003).

Here, we show that lysosomes are also important for the development of B[*a*]P-induced cell death, by regulating both lipid peroxidation and caspase-3 activation. Our data notably demonstrates for the first time the existence of a lysosome-related pathway for caspase-3 activation which is dependent on both iron and endogenous lactoferrin. The present results, together with the findings of our previous works on B[*a*]P-induced cell death in F258 cell line, are summarized in Fig. 8.

Whereas alterations of lysosome morphology, more precisely an increase in compartment size, were expected based upon previous data obtained in B[*a*]P-exposed mussels (Marigomez et al., 2005), our data shows for the first time that these changes are related to B[*a*]P metabolism, since those effects are inhibited by α-NF. Furthermore, we found that B[*a*]P dramatically altered lysosomal pH, a parameter known to be important for the function of these organelles (Palokangas et al., 1994); one must keep in mind that concomitant changes in lysosome morphology and pH have already been reported (Myers et al., 1991). As this change in pH was observed not earlier than 48 h of treatment, this suggested a requirement for metabolism of B[*a*]P. However, we were unable to further test this hypothesis due to effects of α-NF *per se* on lysosomal pH (not shown). Different mechanisms might explain this change in pH: 1) a direct inhibiting effect of B[*a*]P metabolites on the H^+-ATPase, as already described for diverse xenobiotics (Shiraishi et al., 2000; Simon-Plas et al., 1996); 2) a decrease in H^+-ATPase gene expression; or 3) merely a change in H^+ permeability of lysosomal membrane resulting from alterations in physical characteristics, notably due to oxidative stress as observed in various models (Zdolsek and Svensson, 1993). Moreover, mitochondrial ROS production has been shown to induce lysosomal leakage, possibly because of intralysosomal iron-catalyzed oxidative processes (Persson et al., 2003; Dare et al., 2001). In our model, using oligomycin, we found that lysosomal destabilization was indeed linked to mitochondrial dysfunction, thus favouring the hypothesis of a role for mitochondrial ROS production; however, iron would not be involved in these effects since iron chelators did not prevent lysosomal alterations as visualized by AO staining.

B[*a*]P, which is known to interfere with cellular membranes (Jimenez et al., 2002), and to induce bulk membrane fluidization (Gorria et al., 2006b), might induce changes in the lysosomal membrane physical state, which may then participate to lysosomal destabilization. We tried to quantify the membrane physical damages by measuring fluidity of either intracellular vesicles or bulk membrane using a polarization fluorescence technique and TMA-DPH. This probe is indeed useful to study vesicular fluidity *in situ*, since it localizes near the hydrophilic head of the membranes and is consequently easily removable from the plasma membrane, by simply washing the cells (Illinger and Kuhry, 1994). However, in the present study, we were unable to detect any change in membrane fluidity using this probe, whatever the compartment considered, which suggested that membrane fluidity was not affected following B[*a*]P exposure. It is important to note that our previous study showed an increase in bulk membrane fluidity after B[*a*]P treatment (Gorria et al., 2006b); however, in contrast to TMA-DPH, the fluoroprobe used in that study (*i.e.* DPH) is known to localize within the lipophilic inner layer of membranes, thus indicating that the intramembrane space would be more sensitive to B[*a*]P-induced

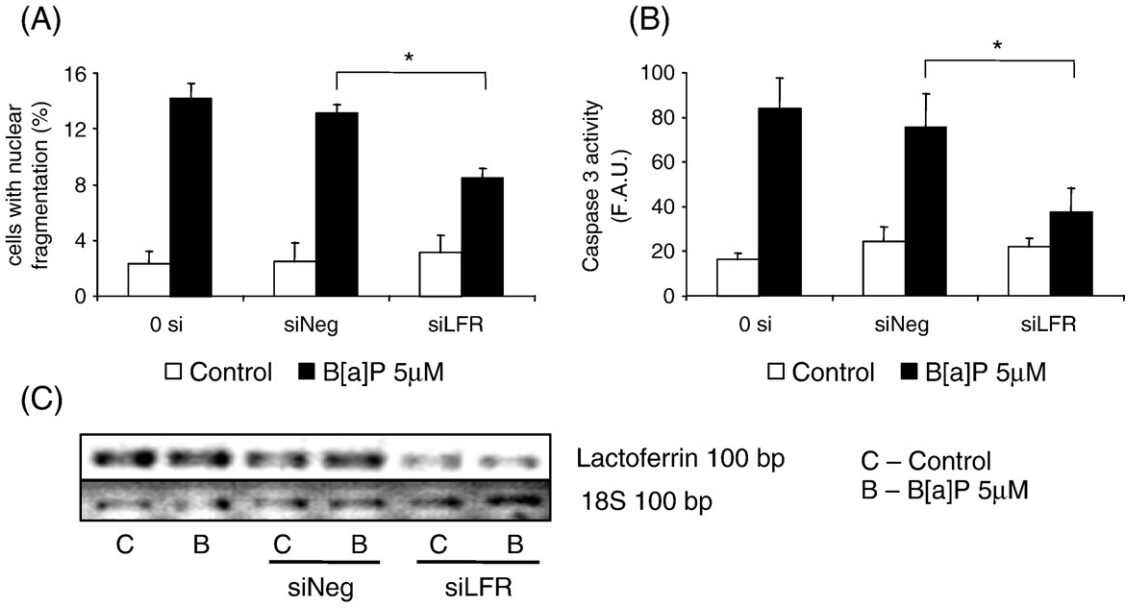

Fig. 7. Lactoferrin is involved in the B[*a*]P-induced cell death *via* the control of caspase activation. (A, B, C) F258 cells were transfected or not (0 si) with siRNA targeting lactoferrin (siLFR) or with negative control siRNA (siNeg), and treated or not (control) with B[*a*]P (5 µM) for 48 h. (A) The percentage of apoptotic cells was analysed by Hoechst 33342 staining. *$p<0.05$ (B) Caspase activity was measured by spectrofluorimetry. F.A.U.: Fluorescence Arbitrary Units. *$p<0.05$. (C) RT-PCR were performed on LFR and ribosomal 18s genes in order to evaluate the efficiency of the siRNAs used. $N=3$ independent experiments for all the protocols tested.

fluidization in our cell model. Unfortunately, DPH could not be used here to measure vesicle fluidity, since this probe is not easily washable when incorporated in membranes. Therefore, a ROS-dependent change in lysosome fluidity upon B[*a*]P, independently of lysosomal iron-dependent lipid peroxidation, is still an open question.

The fact that no general rupture of lysosomal membrane was observed upon B[*a*]P exposure (Fig. 1B), even at a treatment time with marked percentage of cell death, supported the hypothesis that lysosomes may play a role in the related cell death cascade. Using BFM, we did observe an inhibition of cell death. Interestingly, we found that BFM exerted a major effect on caspase-3 activity, thus strongly suggesting the involvement of lysosomes in the activation process of this protease. This observation was very important since under our experimental conditions, neither cytochrome *c*, nor any initiator caspase appears to be involved in the activation of caspase-3 (Huc et al., 2006; Holme et al., 2007).

Recent studies on the involvement of lysosomes in cell death demonstrate that lysosomal destabilization occurs early in the apoptotic cascade, leading to protease leakage within the cytoplasm, thus participating to caspase activation and to mitochondrial dysfunction (reviewed in Brunk et al. (2001); Guicciardi et al. (2004)). In our model, it seems that, in B[*a*]P-treated cells, lysosomes would participate to lipid peroxidation (since inhibited by BFM), together with mitochondria [Gorria and Lagadic-Gossmann, unpublished data]; this thus pointed to the involvement of both lysosomes and mitochondria in the development of oxidative stress. However, B[*a*]P-induced mitochondrial alterations (as visualized by ROS production and intracellular acidification) does not seem to depend on lysosomal dysfunction, since not inhibited by BFM. At the opposite, our data suggested that lysosomal involvement in the apoptotic cascade might be dependent on mitochondria, since inhibited by oligomycin (Fig. 4D).

Puzzled by the fact that BFM partly inhibited lipid peroxidation apparently without inhibiting the mitochondria-dependent ROS production and having previously shown that iron was implicated in the occurrence of lipid peroxidation during B[*a*]P-induced cell death (Gorria et al., 2006a), we further studied the involvement of iron in this cascade. Indeed, iron has been previously shown as capable of inducing lysosomal dysfunction (Persson, 2005). Using two iron chelators with different intracellular localization, we demonstrated first that mitochondrial and lysosomal dysfunctions were not linked to chelatable iron (Figs. 5B and C), and second that the lysosomal pool of iron was essential for caspase-3 activation (Fig. 5A). Two hypotheses might explain such a dependence: 1) a direct effect of iron on caspase activation, as shown for other ions (Pelletier et al., 2005), or 2) its involvement in the activation of proteases implicated in the cleavage of caspase-3. Regarding the former hypothesis, it should be stressed that a recent study showed that caspase-3 *in vitro* was inhibited, rather than activated, by the presence of iron, which might explain why iron chelation by DFO induces apoptosis in some models (Sliskovic and Mutus, 2006). On the other hand, an iron-dependent caspase-3 activation by a sublethal dose of H_2O_2 has also been recently reported (Kumar et al., 2007).

Based upon the fact that both mitochondria-related intracellular acidification (Huc et al., 2006), lysosomal destabilization (Fig. 3B) and lysosomal free iron content (Fig. 5A) were all essential for caspase-3 activation in B[*a*]P-induced apoptosis of F258 cells, we then supposed that some acid requiring lysosomal proteases was involved in caspase-3 cleavage. As cathepsins have largely been shown to mediate caspase-3 activation

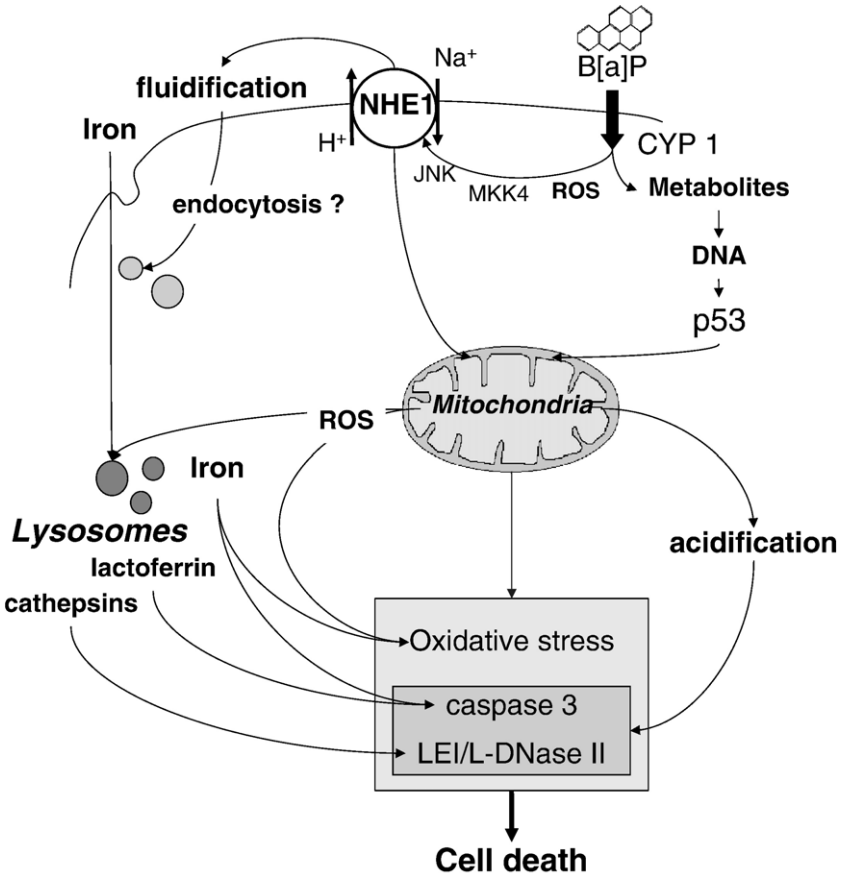

Fig. 8. Schematic summary of the multiple pathways involved in B[*a*]P-induced cell death in the F258 model, and showing the crosstalk which may exist between plasma membrane, mitochondria and lysosomes. B[*a*]P is a lipophilic molecule capable of passively crossing the plasma membrane. In the cytosol, B[*a*]P is metabolized by CYP1 into reactive metabolites and ROS, leading to p53 and NHE1 activation (Huc et al., 2006; Huc et al., 2004). Membrane fluidization upon B[*a*]P treatment is dependent on NHE1 activation and enhances iron uptake, probably through endocytosis (Gorria et al., 2006a, b). During B[*a*]P-induced cell death, lysosomal alterations, more likely through iron (Gorria et al., 2006a), participate to the development of oxidative stress, along with the ROS produced by mitochondria dysfunction [Gorria and Lagadic-Gossmann, unpublished results]. Besides this role, lysosomes appear to be determinant for the triggering of the multiple B[*a*]P-induced cell death cascades, especially through the release of the proteases they contain; these are indeed involved in the activation of both caspase-dependent (lactoferrin, activating caspase-3) and caspase-independent (cathepsins, activating LEI/L-DNase II (Huc et al., 2006)) pathways, which both require the mitochondria-related intracellular acidification (Huc et al., 2006).

(Nagaraj et al., 2006; Johansson et al., 2003, 2006), we first checked their implication in our model and proved that cathepsins were involved in B[*a*]P-induced apoptosis, but not through activation of caspase-3 (Fig. 6) (Huc et al., 2006).

Since we did not find any studies suggesting a role for iron in cathepsin activation, and knowing that iron was essential for caspase-3 activation in our model, we focused on the lysosomal, iron-binding, transferrin protease named lactoferrin (Hendrixson et al., 2003). Interestingly, endogenous lactoferrin has very recently been found to participate in apoptosis through caspase-3 cleavage in D-galactosamine-treated hepatocytes (Katunuma et al., 2006). With the aim of testing whether endogenous lactoferrin was involved in our model, we used a siRNA transfecting protocol in order to silence its expression. Our data clearly demonstrated the essential role of lactoferrin in the increase in caspase-3 activity upon B[*a*]P exposure (Fig. 7A). Compared to Katunuma's work (Katunuma et al., 2006), our data further demonstrated that iron, besides lactoferrin, is essential for caspase-3 activation to occur in cells. If lactoferrin retains iron at a much lower pH than transferrin (pH 3–4, compared with pH 5–6) and has a very high affinity for Fe^{3+} (Baker and Baker, 2005), *in vitro* experiments have nevertheless indicated that iron status would not have any influence on lactoferrin proteolytic activity (Qiu et al., 1998). Therefore, it remains to be understood how iron and lactoferrin could work together to activate caspase-3 in cells.

Conclusion

The present results demonstrate that, upon exposure to the prototype carcinogen B[*a*]P, both lysosomes and mitochondria are involved in creating an intracellular environment (acidification, iron leakage and oxidative stress) necessary for the occurrence of both caspase-dependent (*via* lactoferrin activation) and caspase-independent (*via* cathepsin activation) cell death pathways (Fig. 8). A role for endogenous lactoferrin in caspase-3 activation should deserve future attention in the different models where caspase-3 activation has been shown to occur independently of initiator caspases or cathepsins.

Acknowledgments

The work was supported by the Institut National de la Santé et de la Recherche Médicale (INSERM), the Région Bretagne, Egide (Aurora programme) and the Ligue Nationale contre le Cancer. We wish to thank the microscopy platform and Dr Dutertre (UMR CNRS 6061, IFR 140, Rennes) for the helpful advice on immunolocalization captures and analysis. We also wish to thank Roselyne Primault and Marie-Thérèse Lavault (Département de Microscopie, Faculty of Pharmacy, University of Rennes 1) for the electron microscopy analysis.

References

Baehrecke, E.H., 2005. Autophagy: dual roles in life and death? Nat. Rev., Mol. Cell Biol. 6, 505–510.

Baker, E.N., Baker, H.M., 2005. Molecular structure, binding properties and dynamics of lactoferrin. Cell. Mol. Life Sci. 62, 2531–2539.

Bidere, N., Lorenzo, H.K., Carmona, S., Laforge, M., Harper, F., Dumont, C., Senik, A., 2003. Cathepsin D triggers Bax activation, resulting in selective apoptosis-inducing factor (AIF) relocation in T lymphocytes entering the early commitment phase to apoptosis. J. Biol. Chem. 278, 31401–31411.

Billiard, S.M., Timme-Laragy, A.R., Wassenberg, D.M., Cockman, C., Di Giulio, R.T., 2006. The role of the aryl hydrocarbon receptor pathway in mediating synergistic developmental toxicity of polycyclic aromatic hydrocarbons to zebrafish. Toxicol. Sci. 92, 526–536.

Boya, P., Gonzalez-Polo, R.A., Poncet, D., Andreau, K., Vieira, H.L., Roumier, T., Perfettini, J.L., Kroemer, G., 2003. Mitochondrial membrane permeabilization is a critical step of lysosome-initiated apoptosis induced by hydroxychloroquine. Oncogene 22, 3927–3936.

Broker, L.E., Kruyt, F.A., Giaccone, G., 2005. Cell death independent of caspases: a review. Clin. Cancer Res. 11, 3155–3162.

Brunk, U.T., Svensson, I., 1999. Oxidative stress, growth factor starvation and Fas activation may all cause apoptosis through lysosomal leak. Redox Rep. 4, 3–11.

Brunk, U.T., Dalen, H., Roberg, K., Hellquist, H.B., 1997. Photo-oxidative disruption of lysosomal membranes causes apoptosis of cultured human fibroblasts. Free Radic. Biol. Med. 23, 616–626.

Brunk, U.T., Neuzil, J., Eaton, J.W., 2001. Lysosomal involvement in apoptosis. Redox. Rep. 6, 91–97.

Caruso, J.A., Mathieu, P.A., Joiakim, A., Leeson, B., Kessel, D., Sloane, B.F., Reiners Jr., J.J., 2004. Differential susceptibilities of murine hepatoma 1c1c7 and Tao cells to the lysosomal photosensitizer NPe6: influence of aryl hydrocarbon receptor on lysosomal fragility and protease contents. Mol. Pharmacol. 65, 1016–1028.

Caruso, J.A., Mathieu, P.A., Joiakim, A., Zhang, H., Reiners Jr., J.J., 2006. Aryl hydrocarbon receptor modulation of tumor necrosis factor-alpha-induced apoptosis and lysosomal disruption in a hepatoma model that is caspase-8-independent. J. Biol. Chem. 281, 10954–10967.

Cirman, T., Oresic, K., Mazovec, G.D., Turk, V., Reed, J.C., Myers, R.M., Salvesen, G.S., Turk, B., 2004. Selective disruption of lysosomes in HeLa cells triggers apoptosis mediated by cleavage of Bid by multiple papain-like lysosomal cathepsins. J. Biol. Chem. 279, 3578–3587.

Dare, E., Li, W., Zhivotovsky, B., Yuan, X., Ceccatelli, S., 2001. Methylmercury and H(2)O(2) provoke lysosomal damage in human astrocytoma D384 cells followed by apoptosis. Free Radic. Biol. Med. 30, 1347–1356.

Eskelinen, E.L., 2005. Maturation of autophagic vacuoles in mammalian cells. Autophagy 1, 1–10.

Ferri, K.F., Kroemer, G., 2001. Organelle-specific initiation of cell death pathways. Nat. Cell Biol. 3, E255–E263.

Gilot, D., Loyer, P., Corlu, A., Glaise, D., Lagadic-Gossmann, D., Atfi, A., Morel, F., Ichijo, H., Guguen-Guillouzo, C., 2002. Liver protection from apoptosis requires both blockage of initiator caspase activities and inhibition of ASK1/JNK pathway via glutathione S-transferase regulation. J. Biol. Chem. 277, 49220–49229.

Glickstein, H., El, R.B., Shvartsman, M., Cabantchik, Z.I., 2005. Intracellular labile iron pools as direct targets of iron chelators: a fluorescence study of chelator action in living cells. Blood 106, 3242–3250.

Gorria, M., Huc, L., Sergent, O., Rebillard, A., Gaboriau, F., Dimanche-Boitrel, M.T., Lagadic-Gossmann, D., 2006a. Protective effect of monosialoganglioside GM1 against chemically-induced apoptosis through targeting of mitochondrial function and iron transport. Biochem. Pharmacol. 72, 1343–1353.

Gorria, M., Tekpli, X., Sergent, O., Huc, L., Gaboriau, F., Rissel, M., Chevanne, M., Dimanche-Boitrel, M.T., Lagadic-Gossmann, D., 2006b. Membrane fluidity changes are associated with benzo[a]pyrene-induced apoptosis in F258 cells: protection by exogenous cholesterol. Ann. N.Y. Acad. Sci. 1090, 108–112.

Guicciardi, M.E., Leist, M., Gores, G.J., 2004. Lysosomes in cell death. Oncogene 23, 2881–2890.

Hait, W.N., Jin, S., Yang, J.M., 2006. A matter of life or death (or both): understanding autophagy in cancer. Clin. Cancer Res. 12, 1961–1965.

Heming, T.A., Traber, D.L., Hinder, F., Bidani, A., 1995. Effects of bafilomycin A1 on cytosolic pH of sheep alveolar and peritoneal macrophages: evaluation of the pH-regulatory role of plasma membrane V-ATPases. J. Exp. Biol. 198, 1711–1715.

Hendrixson, D.R., Qiu, J., Shewry, S.C., Fink, D.L., Petty, S., Baker, E.N., Plaut, A.G., St Geme III, J.W., 2003. Human milk lactoferrin is a serine protease that cleaves *Haemophilus* surface proteins at arginine-rich sites. Mol. Microbiol. 47, 607–617.

Holme, J.A., Gorria, M., Arlt, V.M., Ovrebo, S., Solhaug, A., Tekpli, X., Landvik, N.E., Huc, L., Fardel, O., Lagadic-Gossmann, D., 2007. Different mechanisms involved in apoptosis following exposure to benzo[a]pyrene in F258 and Hepa1c1c7 cells. Chem. Biol. Interact 167, 41–55.

Huc, L., Sparfel, L., Rissel, M., Dimanche-Boitrel, M.T., Guillouzo, A., Fardel, O., Lagadic-Gossmann, D., 2004. Identification of Na+/H+ exchange as a new target for toxic polycyclic aromatic hydrocarbons. FASEB J. 18, 344–346.

Huc, L., Rissel, M., Solhaug, A., Tekpli, X., Gorria, M., Torriglia, A., Holme, J.A., Dimanche-Boitrel, M.T., Lagadic-Gossmann, D., 2006. Multiple apoptotic pathways induced by p53-dependent acidification in benzo[a]pyrene-exposed hepatic F258 cells. J. Cell. Physiol. 208, 527–537.

Huc, L., Tekpli, X., Holme, J.A., Rissel, M., Solhaug, A., Gardyn, C., Le Moigne, G., Gorria, M., Dimanche-Boitrel, M.T., Lagadic-Gossmann, D., 2007. c-Jun NH2-terminal kinase-related Na+/H+ exchanger isoform 1 activation controls hexokinase II expression in benzo(a)pyrene-induced apoptosis. Cancer Res. 67, 1696–1705.

Illinger, D., Kuhry, J.G., 1994. The kinetic aspects of intracellular fluorescence labeling with TMA-DPH support the maturation model for endocytosis in L929 cells. J. Cell Biol. 125, 783–794.

Ishisaka, R., Utsumi, T., Kanno, T., Arita, K., Katunuma, N., Akiyama, J., Utsumi, K., 1999. Participation of a cathepsin L-type protease in the activation of caspase-3. Cell Struct. Funct. 24, 465–470.

Jia, L., Dourmashkin, R.R., Allen, P.D., Gray, A.B., Newland, A.C., Kelsey, S.M., 1997. Inhibition of autophagy abrogates tumour necrosis factor alpha induced apoptosis in human T-lymphoblastic leukaemic cells. Br. J. Haematol. 98, 673–685.

Jimenez, M., Aranda, F.J., Teruel, J.A., Ortiz, A., 2002. The chemical toxic benzo[a]pyrene perturbs the physical organization of phosphatidylcholine membranes. Environ. Toxicol. Chem. 21, 787–793.

Johansson, A.C., Steen, H., Ollinger, K., Roberg, K., 2003. Cathepsin D mediates cytochrome *c* release and caspase activation in human fibroblast apoptosis induced by staurosporine. Cell Death Differ. 10, 1253–1259.

Johansson, A.C., Norberg-Spaak, L., Roberg, K., 2006. Role of lysosomal cathepsins in naphthazarin- and Fas-induced apoptosis in oral squamous cell carcinoma cells. Acta Otolaryngol. 126, 70–81.

Kanzawa, T., Germano, I.M., Komata, T., Ito, H., Kondo, Y., Kondo, S., 2004. Role of autophagy in temozolomide-induced cytotoxicity for malignant glioma cells. Cell Death Differ. 11, 448–457.

Katunuma, N., Le, Q.T., Murata, E., Matsui, A., Majima, E., Ishimaru, N., Hayashi, Y., Ohashi, A., 2006. A novel apoptosis cascade mediated by lysosomal lactoferrin and its participation in hepatocyte apoptosis induced by D-galactosamine. FEBS Lett. 580, 3699–3705.

Katunuma, N., Murata, E., Le, Q.T., Hayashi, Y., Ohashi, A., 2004. New apoptosis cascade mediated by lysosomal enzyme and its protection by epigallo-catechin gallate. Adv. Enzyme Regul. 44, 1–10.

Kessel, D., Luo, Y., Mathieu, P., Reiners Jr., J.J., 2000. Determinants of the apoptotic response to lysosomal photodamage. Photochem. Photobiol. 71, 196–200.

Kroemer, G., Jaattela, M., 2005. Lysosomes and autophagy in cell death control. Nat. Rev., Cancer 5, 886–897.

Kumar, A.P., Chang, M.K., Fliegel, L., Pervaiz, S., Clement, M.V., 2007. Oxidative repression of NHE1 gene expression involves iron-mediated caspase activity. Cell Death Differ. 14, 1733–1746.

Lin, T.Y., Chiou, S.H., Chen, M., Kuo, C.D., 2005. Human lactoferrin exerts bi-directional actions on PC12 cell survival via ERK1/2 pathway. Biochem. Biophys. Res. Commun. 337, 330–336.

Marchi, B., Burlando, B., Moore, M.N., Viarengo, A., 2004. Mercury- and copper-induced lysosomal membrane destabilisation depends on [Ca2+]i dependent phospholipase A2 activation. Aquat. Toxicol. 66, 197–204.

Marigomez, I., Izagirre, U., Lekube, X., 2005. Lysosomal enlargement in digestive cells of mussels exposed to cadmium, benzo[a]pyrene and their combination. Comp. Biochem. Physiol., C Toxicol. Pharmacol. 141, 188–193.

Mozhenok, T., Belyaeva, T., Bulychev, A., Kuznetsova, I., Leontieva, E., Faddejeva, M., 1998. Effects of some biologically active compounds on phagosome–lysosome fusion in peritoneal macrophages of mice. Cell Biol. Int. 22, 465–472.

Myers, B.M., Prendergast, F.G., Holman, R., Kuntz, S.M., LaRusso, N.F., 1991. Alterations in the structure, physicochemical properties, and pH of hepatocyte lysosomes in experimental iron overload. J. Clin. Invest. 88, 1207–1215.

Nagaraj, N.S., Vigneswaran, N., Zacharias, W., 2006. Cathepsin B mediates TRAIL-induced apoptosis in oral cancer cells. J. Cancer Res. Clin. Oncol. 132, 171–183.

Ono, K., Kim, S.O., Han, J., 2003. Susceptibility of lysosomes to disruption is a determinant for plasma membrane disruption in tumor necrosis factor alpha-induced cell death. Mol. Cell. Biol. 23, 665–676.

Palokangas, H., Metsikko, K., Vaananen, K., 1994. Active vacuolar H+ ATPase is required for both endocytic and exocytic processes during viral infection of BHK-21 cells. J. Biol. Chem. 269, 17577–17585.

Paquet, C., Sane, A.T., Beauchemin, M., Bertrand, R., 2005. Caspase- and mitochondrial dysfunction-dependent mechanisms of lysosomal leakage and cathepsin B activation in DNA damage-induced apoptosis. Leukemia 19, 784–791.

Pelletier, M., Oliver, L., Meflah, K., Vallette, F.M., 2005. Caspase-3 can be pseudo-activated by a Ca2+-dependent proteolysis at a non-canonical site. FEBS Lett. 579, 2364–2368.

Persson, H.L., 2005. Iron-dependent lysosomal destabilization initiates silica-induced apoptosis in murine macrophages. Toxicol. Lett. 159, 124–133.

Persson, H.L., Yu, Z., Tirosh, O., Eaton, J.W., Brunk, U.T., 2003. Prevention of oxidant-induced cell death by lysosomotropic iron chelators. Free Radic. Biol. Med. 34, 1295–1305.

Petrat, F., de Groot, H., Rauen, U., 2001. Subcellular distribution of chelatable iron: a laser scanning microscopic study in isolated hepatocytes and liver endothelial cells. Biochem. J. 356, 61–69.

Qiu, J., Hendrixson, D.R., Baker, E.N., Murphy, T.F., St Geme III, J.W., Plaut, A.G., 1998. Human milk lactoferrin inactivates two putative colonization factors expressed by *Haemophilus influenzae*. Proc. Natl. Acad. Sci. U. S. A. 95, 12641–12646.

Roberg, K., Johansson, U., Ollinger, K., 1999. Lysosomal release of cathepsin D precedes relocation of cytochrome *c* and loss of mitochondrial transmembrane potential during apoptosis induced by oxidative stress. Free Radic. Biol. Med. 27, 1228–1237.

Schafer, F.Q., Buettner, G.R., 2000. Acidic pH amplifies iron-mediated lipid peroxidation in cells. Free Radic. Biol. Med. 28, 1175–1181.

Shiraishi, Y., Nagai, J., Murakami, T., Takano, M., 2000. Effect of cisplatin on H+ transport by H+-ATPase and Na+/H+ exchanger in rat renal brush-border membrane. Life Sci. 67, 1047–1058.

Simon-Plas, F., Gomes, E., Milat, M.L., Pugin, A., Blein, J.P., 1996. Cercospora beticola toxins (X. Inhibition of plasma membrane H+-ATPase by beticolin-1). Plant Physiol. 111, 773–779.

Singh, J.K., Dasgupta, A., Adayev, T., Shahmehdi, S.A., Hammond, D., Banerjee, P., 1996. Apoptosis is associated with an increase in saturated fatty acid containing phospholipids in the neuronal cell line, HN2-5. Biochim. Biophys. Acta 1304, 171–178.

Sliskovic, I., Mutus, B., 2006. Reversible inhibition of caspase-3 activity by iron (III) Potential role in physiological control of apoptosis. FEBS. Lett. 580, 2233–2237.

Solhaug, A., Refsnes, M., Lag, M., Schwarze, P.E., Husoy, T., Holme, J.A., 2004. Polycyclic aromatic hydrocarbons induce both apoptotic and anti-apoptotic signals in Hepa1c1c7 cells. Carcinogenesis 25, 809–819.

Solhaug, A., Ovrebo, S., Mollerup, S., Lag, M., Schwarze, P.E., Nesnow, S., Holme, J.A., 2005. Role of cell signaling in B[a]P-induced apoptosis: characterization of unspecific effects of cell signaling inhibitors and apoptotic effects of B[a]P metabolites. Chem. Biol. Interact. 151, 101–119.

Sparfel, L., Van Grevenynghe, J., Le Vee, M., Aninat, C., Fardel, O., 2006. Potent inhibition of carcinogen-bioactivating cytochrome P450 1B1 by the p53 inhibitor pifithrin alpha. Carcinogenesis 27, 656–663.

Taha, T.A., Kitatani, K., Bielawski, J., Cho, W., Hannun, Y.A., Obeid, L.M., 2005. Tumor necrosis factor induces the loss of sphingosine kinase-1 by a cathepsin B-dependent mechanism. J. Biol. Chem. 280, 17196–17202.

Tapper, H., Sundler, R., 1995. Bafilomycin A1 inhibits lysosomal, phagosomal, and plasma membrane H(+)-ATPase and induces lysosomal enzyme secretion in macrophages. J. Cell. Physiol. 163, 137–144.

Turk, B., Stoka, V., Rozman-Pungercar, J., Cirman, T., Droga-Mazovec, G., Oresic, K., Turk, V., 2002. Apoptotic pathways: involvement of lysosomal proteases. Biol. Chem. 383, 1035–1044.

Uchimoto, T., Nohara, H., Kamehara, R., Iwamura, M., Watanabe, N., Kobayashi, Y., 1999. Mechanism of apoptosis induced by a lysosomotropic agent, L-Leucyl-L-Leucine methyl ester. Apoptosis 4, 357–362.

Vancompernolle, K., Van Herreweghe, F., Pynaert, G., Van de Craen, M., De Vos, K., Totty, N., Sterling, A., Fiers, W., Vandenabeele, P., Grooten, J., 1998. Atractyloside-induced release of cathepsin B, a protease with caspase-processing activity. FEBS Lett. 438, 150–158.

Wan, F.Y., Wang, Y.N., Zhang, G.J., 2002. Influence of the physical states of membrane surface area and center area on lysosomal proton permeability. Arch. Biochem. Biophys. 404, 285–292.

Wang, J., Zhang, G.J., 2005. Influence of membrane physical state on lysosomal potassium ion permeability. Cell. Biol. Int. 29, 393–401.

Yang, L., Zhang, G.J., Zhong, Y.G., Zheng, Y.Z., 2000. Influence of membrane fluidity modifiers on lysosomal osmotic sensitivity. Cell. Biol. Int. 24, 699–704.

Yin, L., Stearns, R., Gonzalez-Flecha, B., 2005. Lysosomal and mitochondrial pathways in H2O2-induced apoptosis of alveolar type II cells. J. Cell. Biochem. 94, 433–445.

Yu, Z., Persson, H.L., Eaton, J.W., Brunk, U.T., 2003. Intralysosomal iron: a major determinant of oxidant-induced cell death. Free Radic. Biol. Med. 34, 1243–1252.

Yuan, X.M., Li, W., Dalen, H., Lotem, J., Kama, R., Sachs, L., Brunk, U.T., 2002. Lysosomal destabilization in p53-induced apoptosis. Proc. Natl. Acad. Sci. U. S. A. 99, 6286–6291.

Zdolsek, J.M., Svensson, I., 1993. Effect of reactive oxygen species on lysosomal membrane integrity. A study on a lysosomal fraction. Virchows Arch., B Cell. Pathol. Incl. Mol. Pathol. 64, 401–406.

Zhang, G.J., Liu, H.W., Yang, L., Zhong, Y.G., Zheng, Y.Z., 2000. Influence of membrane physical state on the lysosomal proton permeability. J. Membr. Biol. 175, 53–62.

Zhao, M., Antunes, F., Eaton, J.W., Brunk, U.T., 2003. Lysosomal enzymes promote mitochondrial oxidant production, cytochrome c release and apoptosis. Eur. J. Biochem. 270, 3778–3786.